Differences in image-enhanced endoscopic findings between *Helicobacter pylori*-associated and autoimmune gastritis ▶

OPEN ACCESS

Authors

Minoru Kato[1], Noriya Uedo[1], Ervin Toth[2], Satoki Shichijo[1], Akira Maekawa[1], Takashi Kanesaka[1], Yoji Takeuchi[1], Sachiko Yamamoto[1], Koji Higashino[1], Ryu Ishihara[1], Artur Nemeth[2], Henrik Thorlacius[3], Yasuhiko Tomita[4,5], Gabriele Wurm Johansson[2]

Institutions

1　Department of Gastrointestinal Oncology, Osaka International Cancer Institute, Osaka, Japan
2　Department of Endoscopy, Skåne University Hospital, Lund University, Malmö, Sweden
3　Department of Surgery, Skåne University Hospital, Lund University, Malmö, Sweden
4　Department of Pathology, Osaka International Cancer Institute, Osaka, Japan
5　Department of Pathology, International University of Health and Welfare, Japan

Corresponding author
Noriya Uedo, MD, Department of Gastrointestinal Oncology, Osaka International Cancer Institute, 1-69, Otemae 3-Chome, Chuo-ku, Osaka, 541-8567, Japan
Fax: +81-6-6981-4067
noriya.uedo@gmail.com

ABSTRACT

Background and study aims　The aim of this study was to elucidate the differences in image-enhanced endoscopy (IEE) findings between *Helicobacter-pylori*-associated and autoimmune gastritis.

Patients and methods　Seven *H. pylori*-naïve, 21 patients with *H. pylori*-associated gastritis and seven with autoimmune gastritis were enrolled. Mucosal atrophy in the corpus was evaluated using autofluorescence imaging and classified into small, medium and large. In a 2×2-cm area of the lesser curvature of the lower corpus, micromucosal pattern was evaluated by magnifying narrow band imaging and proportion of foveola (FV)- and groove (GR)-type mucosa was classified into FV>80%, FV 50% to 80%, GR 50% to 80%, and GR>80%, then a biopsy specimen was taken.

Results　Fifteen of 21 (71%) *H. pylori*-associated gastritis patients exhibited medium-to-large atrophic mucosa at the corpus lesser curvature. All autoimmune gastritis patients had large atrophic mucosa throughout the corpus (P <0.001). All *H. pylori*-naïve patients had the FV>80% micromucosal pattern. Nineteen of 21 (90%) *H. pylori*-associated gastritis patients had varying proportions of GR- and FV-type mucosae and five of seven (71%) autoimmune gastritis patients showed FV>80% mucosa (P<0.001). Compared with patients who were *H. pylori*-naïve, patients with *H. pylori*-associated and autoimmune gastritis exhibited a higher grade of atrophy (P<0.001), but only patients with *H. pylori*-associated gastritis showed a higher grade of intestinal metaplasia (P=0.022). Large mucosal atrophy with FV>80% micromucosal pattern had sensitivity of 71% (95% CI: 29%–96%) and specificity of 100% (95% CI: 88% to 100%) for diagnosis of autoimmune gastritis.

Conclusions　IEE findings of the gastric corpus differed between *H. pylori*-associated and autoimmune gastritis, suggesting different pathogenesis of the two diseases.

Introduction

Helicobacter-pylori-associated gastritis and autoimmune gastritis are two major types of chronic atrophic gastritis [1]. *H. pylori*-associated gastritis increases the incidence of gastroduodenal ulcer [2], gastric adenoma, gastric cancer [3, 4], and mucosa-associated lymphoid tissue lymphoma in the stomach [5]. Autoimmune gastritis increases development of iron-deficiency anemia [6], pernicious anemia [7], and gastric neuroendocrine tumor (NET) [8]. Discrimination of these two types of gastritis is important to understand the risk of different diseases that may develop in patients with atrophic gastritis. The classical endoscopic findings for autoimmune gastritis are corpus mucosal atrophy and minimal mucosal change in the antrum. However, it is often difficult to diagnose autoimmune gastritis by white-light endoscopy alone.

Image-enhanced endoscopy (IEE) is designed to enhance mucosal characteristics and improve diagnostic yield of endoscopy for various diseases of the digestive tract [9, 10]. Autofluorescence imaging (AFI) displays the extent of histological mucosal atrophy in the gastric corpus as a greenish color, with sensitivity of 72 % and specificity of 78 % [11]. Magnifying narrow-band imaging (NBI) enables us to observe detailed micromucosal findings of the gastric mucosa that represent histological features of *H. pylori*-associated gastritis [12–15]. However, so far, there have been a few case reports but no systematic investigation of IEE findings of autoimmune gastritis [16, 17].

The aim of the present study was to elucidate the differences in IEE findings between *H. pylori*-associated and autoimmune gastritis.

Patients and methods

Study design and setting

This was an observational study conducted at a cancer referral hospital, Osaka International Cancer Institute, Osaka, Japan and Skåne University Hospital, Lund University, Malmö, Sweden between April 2014 and July 2015. The study protocol was approved by the Institutional Review Board, Osaka International Cancer Institution on March 26, 2014 (No. 1403265240). The study was registered in the University Hospital Medical Information Network Center as UMIN000019392.

Participants

Patients undergoing esophagogastroduodenoscopy for the following indications were eligible for inclusion: 1) screening for gastric cancer; 2) dyspeptic symptoms; 3) surveillance after endoscopic treatment of early gastric cancer; 4) surveillance after endoscopic treatment of NET; and 5) pernicious anemia. Patients were excluded if they had: 1) a history of *H. pylori* eradication therapy; 2) anticoagulation therapy or coagulopathy; 3) treatment with nonsteroidal anti-inflammatory drugs or steroids; 4) a history of esophagogastric surgery; or 5) major organ failure.

Patients who met inclusion criteria, did not fulfil exclusion criteria, and gave written informed consent for study participation were tested for serum anti-*H. pylori* antibody (E-plate test,

Eiken Chemical, Co, Ltd, Japan) and gastrin levels, then underwent endoscopic examination according to the protocol below. Among them, those who satisfied diagnostic criteria of *H. pylori*-naïve, *H. pylori*-associated gastritis, and autoimmune gastritis were enrolled for analysis in this study.

Endoscopic procedure

Endoscopic examinations were performed using a trimodal imaging endoscopy system that consisted of a light source (CLV-260SL or CLV-290SL; Olympus Medical Systems, Tokyo, Japan), image processor (CV-260SL or CV-290; Olympus), and a magnifying videoendoscope (GIF-FQ260Z; Olympus) that was equipped with two charged coupled devices: one for high-definition white-light imaging (WLI) and NBI modes with zoom function, and another for AFI mode. A black rubber cap (MAJ-1990; Olympus) was fitted to the tip of the videoendoscope for magnifying observation. Structural enhancement level was set at B6 in WLI, B8 in NBI, and A3 in AFI modes. The patients ingested a mixture consisting of a mucolytic agent (20,000 U pronase, Pronase MS; Kaken Pharmaceutical, Tokyo, Japan), defoaming agent (80 mg dimethylpolysiloxane syrup, Gascon Drops; Kissei Pharmaceutical, Matsumoto, Japan), and 1 g sodium bicarbonate diluted in 40 mL water.

After standard observation of the esophagus, stomach and duodenum by WLI, the following endoscopic procedures were performed. First, the extent of atrophic mucosa was evaluated by AFI [11]. For evaluation, the lumen of the gastric corpus was adequately distended with air insufflation to obtain sufficient mucosal images. Next, micromucosal pattern of the lesser curvature of the lower corpus was assessed by magnifying NBI [15]. The region of interest to investigate the micromucosal patterns measured 2×2 cm at the corpus lesser curvature, 4 cm proximal to the gastric angulus. Finally, a biopsy specimen was taken from the center of the region of interest. The reason why we decided this region-of-interest was because, in patients with *H. pylori* associated gastritis, atrophic gastritis usually starts from the lesser curvature of the lower corpus [18]. Therefore, we assumed that mucosal findings of *H. pylori* associated gastritis develop early in this area and change according to the progression of atrophic gastritis [15]. Systematic biopsies, two each from the lesser and greater curvatures of the antrum and two each from the lesser and greater curvatures of the corpus, were taken according to the updated Sydney system [1].

An endoscopist (N.U.) who had experience with AFI and magnifying NBI observation in more than 1000 cases performed all the endoscopic procedures. The findings of AFI and magnifying NBI were determined on-site during the procedure and were input in a spreadsheet computer software.

Extent of atrophic mucosa in AFI

The extent of atrophic mucosa was examined in AFI mode, and was classified into six categories according to the Kimura–Takemoto classification [11, 19]: C-I, the entire gastric body looked purple to dark green; C-II, a color border on the lesser curvature was observed at a lower part of the gastric body; C-III, a color border on the lesser curvature was observed at an upper part of the gastric body; O-I, color borders were observed between
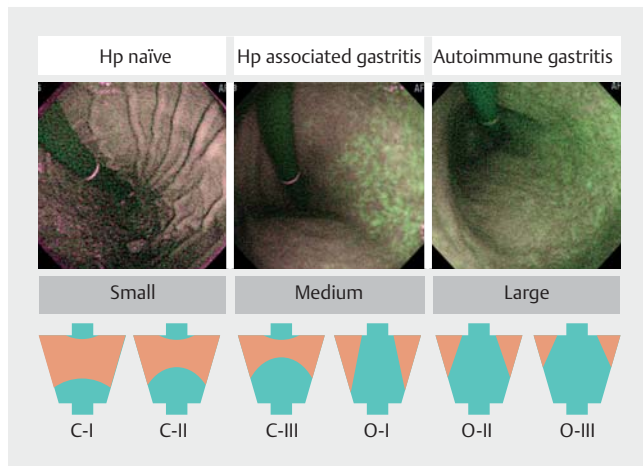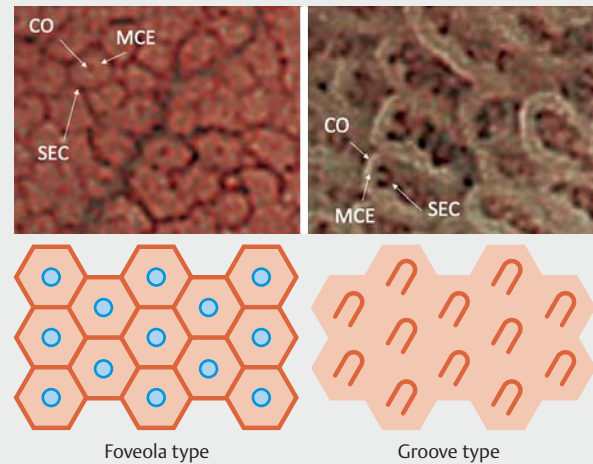
► **Fig. 1** Classification of the extent of atrophic mucosa in autofluorescence imaging. Image of *Helicobacter pylori* (*H. pylori*)-naïve patient (left): a small area of green mucosa was observed in the lower part of the corpus lesser curvature. Image of *H. pylori*-associated gastritis patient (middle): green mucosa was present in the lesser curvature. Image of autoimmune gastritis patient (right): large green mucosa was seen in the corpus. Corresponding illustrations of Kimura–Takemoto classification (C-I to O-III) are shown below.

► **Fig. 2** Two types of micromucosal patterns observed in magnifying narrow-band imaging (upper), and schematic diagram of these structures (lower). The foveola-type mucosa (left) was defined as round, regular crypt-opening (CO) and marginal crypt epithelium (MCE) surrounded by a network of brownish subepithelial capillaries (SEC). The groove-type mucosa (right) was defined as brownish SECs surrounded by ridged MCE.

the lesser curvature and the anterior/posterior wall; O-II, color borders were observed between the anterior/posterior wall and the greater curvature; and O-III, a color border on the greater curvature was observed proximal to the lower gastric body. The extent of atrophic mucosa was regarded as small for C-I and C-II, medium for C-III and O-I, and large for O-II and O-III (► **Fig. 1**). The AFI shows good interobserver agreement ($\kappa = 0.66$) for diagnosis of the extent of atrophic mucosa [11].

Micromucosal pattern in magnifying NBI

Micromucosal pattern of the region of interest was evaluated by magnifying NBI and it was categorized into foveola- and groove-types [15]. The foveola-type mucosa was characterized by round-to-oval, regular crypt openings and marginal crypt epithelium that was surrounded by a network of brownish subepithelial capillaries. Groove-type was defined as mucosa with brownish subepithelial capillaries encased in the crest of marginal crypt epithelium that was divided by continuous grooves of crypt openings (► **Fig. 2**). According to proportion of foveola- and groove-type mucosa, micromucosal pattern in the region of interest was classified into >80 % foveola, 50 % to 80 % foveola, 50 % to 80 % groove, and >80 % groove type mucosa. The magnifying NBI has good interobserver agreement ($\kappa > 0.75$) for diagnosis of gastric mucosal pattern [20].

All of the biopsy specimens were stained with hematoxylin and eosin. Mononuclear cell infiltration (inflammation), neutrophil infiltration (activity), glandular atrophy (atrophy), and intestinal metaplasia were estimated and graded as normal, mild, moderate or marked [1]. The histological findings were evaluated by one pathologist who was unaware of the endoscopic findings.

Diagnosis of *H. pylori*-naïve patients and *H. pylori*-associated gastritis

Diagnosis of *H. pylori*-naïve patients and *H. pylori*-associated gastritis was made by serum anti-*H. pylori* antibody test and histological findings of systematically taken biopsy specimens from gastric mucosa according to the updated Sydney system [1]. Patients with serum anti-*H. pylori* antibody titer <3 U/mL and histologically normal gastric mucosa in all biopsy specimens were diagnosed as *H. pylori*-naïve. Patients with serum anti-*H. pylori* antibody titer ≥10 U/mL or presence of *H. pylori*-like organisms in any biopsy specimens were diagnosed with *H. pylori*-associated gastritis.

Diagnosis of autoimmune gastritis

Patients fulfilling all the following conditions were diagnosed with autoimmune gastritis: 1) serum anti-*H. pylori* antibody titer <3 U/mL and no *H. pylori*-like organisms in all biopsy specimens; 2) clinical manifestations consistent with autoimmune gastritis, such as gastric NET, or pernicious anemia; and 3) biopsy findings of nonatrophic antral mucosa and inflamed atrophic corpus mucosa.

Statistical analysis

The prevalence of foveola-type micromucosal pattern in the corpus mucosa in autoimmune gastritis and *H. pylori*-associated gastritis patients were assumed as 80 % and 20 %, respectively, based on clinical experience of a primary investigator (N.U.). As a result of the rarity of autoimmune gastritis, we set the sample size ratio as 1:3. A required sample size of six was calculated for autoimmune gastritis and 18 for *H. pylori*-associated gastritis, with statistical power of 80 % and two-sided signifi-

	H. pylori-naïve (n = 7)	H. pylori-associated gastritis (n = 21)	Autoimmune gastritis (n = 7)	P value
Median age (range), y	54 (48–70)	73 (49–84)	69 (39–75)	0.032
Sex				0.678
▪ Male	3	10	2	
▪ Female	4	11	5	
Country				0.054
▪ Japan	6	21	5	
▪ Sweden	1	0	2	
Indication for EGD				<0.001
▪ Screening	5	12	0	
▪ Dyspepsia	2	3	0	
▪ Surveillance for EGC	0	6	0	
▪ Surveillance for NET	0	0	5	
▪ Pernicious anemia	0	0	2	
Median serum gastrin level (25th–75th percentile, pg/mL)	Not evaluated	178 (96–563)	2560 (1635–6015)	0.007

EGC, early gastric cancer; EGD, esophagogastroduodenoscopy; NET, neuroendocrine tumor.

cance level of 5% [21]. After considering the possibility of missing values, we planned to enroll seven autoimmune gastritis and 21 *H. pylori*-associated gastritis patients. As a control for normal gastric mucosa, we included seven *H. pylori*-naïve patients.

For comparisons, a chi-square test was used for categorical variables and a Wilcoxon/Kruskal–Wallis test was used for numerical variables. JMP version 15.1.0 software (SAS Institute, Cary, NC, USA) was used for statistical analyses. $P < 0.05$ was considered to be statistically significant.

Results

Patient demographics are listed in ► **Table 1**. There were significant differences in age, indication for esophagogastroduodenoscopy, and serum gastrin level among the groups. Median serum gastrin level in autoimmune gastritis patients was 2560 pg/mL.

► **Table 2** summarizes the IEE appearance of the gastric corpus in AFI mode and magnifying NBI. The corpus mucosa of all patients who were *H. pylori*-naïve was purple in AFI. Fifteen of 21 patients (71%) with *H. pylori*-associated gastritis had medium-to-large green atrophic mucosa predominantly in the lesser curvature. All autoimmune gastritis patients had a large area of green atrophic mucosa throughout the corpus ($P < 0.001$, ► **Fig. 1**). The micromucosal pattern of all *H. pylori*-naïve patients was all foveola-type. Nineteen of 21 patients (90%) with *H. pylori*-associated gastritis had varying proportions of groove- and foveola-type mucosa. Five of seven patients (71%) with autoimmune gastritis had the >80% foveola-type mucosa that was

similar to that in patients who were *H. pylori*-naïve ($P = 0.001$) (► **Fig. 3**, ► **Video 1**). When diagnostic criteria for autoimmune gastritis were defined as a large area (O-II or O-III) of endoscopic atrophy with >80% foveola-type mucosa in the corpus, sensitivity was 71% [95% confidence interval (CI): 29%-96%] (5/7 cases), specificity was 100% (95% CI: 88%-100%) (28/28 cases), and accuracy was 94% (95% CI: 81%-99%) (33/35 cases), respectively. Among patients with *H. pylori*-associated gastritis with a large atrophic mucosa (n = 4), none had a >80% foveola-type micromucosal pattern in magnifying NBI images.

Histological biopsy findings are shown in ► **Table 3**. In one patient with autoimmune gastritis, biopsy specimens were not obtained. Patients with *H. pylori*-gastritis and autoimmune gastritis had significantly higher-grade of inflammation ($P < 0.001$) and atrophy ($P < 0.001$) in the corpus mucosa than patients who were *H. pylori*-naïve. However, intestinal metaplasia was only seen in patients with *H. pylori*-associated gastritis (► **Fig. 4**).

Discussion

In this study, we demonstrated different IEE appearances of gastric corpus mucosa between *H. pylori*-associated gastritis and autoimmune gastritis.

H. pylori-associated gastritis showed lesser curvature predominant endoscopic atrophy in the corpus mucosa in AFI mode. The Kimura and Takemoto classification characterizes endoscopic atrophic mucosa as having a pale color, increased vessel visibility, and low mucosal height [19], and classifies its extent into six patterns from C-I to O-III. AFI showed the endoscopic atrophic mucosa defined by Kimura and Takemoto as a green

▶Table 2 Endoscopic appearance of gastric corpus.

	H. pylori-naïve (n = 7)	*H. pylori*-associated gastritis (n = 21)	Autoimmune gastritis (n = 7)	*P* value
Extent of atrophy in AFI				< 0.001
▪ Small	7	6	0	
▪ Medium	0	11	0	
▪ Large	0	4	7	
Micromucosal pattern in magnifying NBI				0.001
▪ FV > 80 %	7	2	5	
▪ FV 50 %–80 %	0	8	1	
▪ GR 50 %–80 %	0	6	1	
▪ GR > 80 %	0	5	0	

AFI, autofluorescence imaging; FV, foveola; GR, groove; NBI, narrow-band imaging.
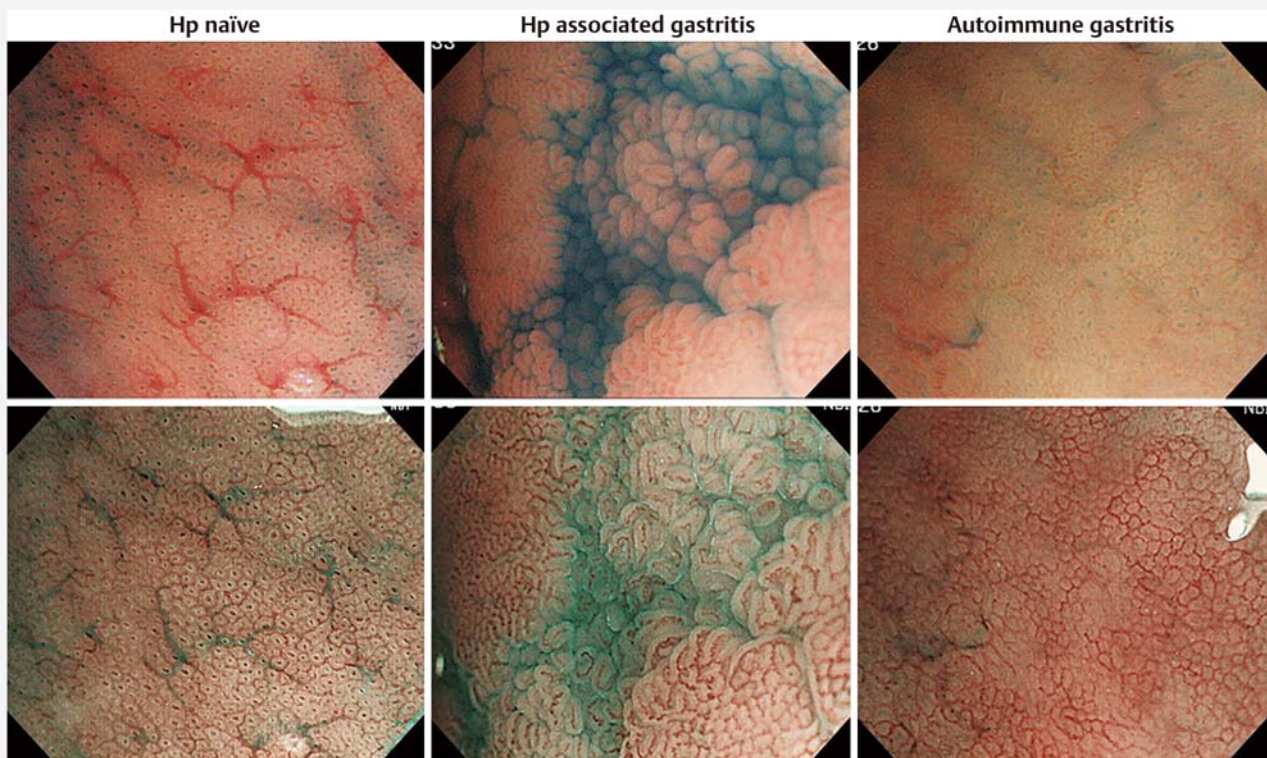
▶Fig. 3 Micromucosal patterns seen in magnifying chromoendoscopy and narrow-band imaging (NBI) in each patient group. Images from *Helicobacter pylori* (*H. pylori*)-naïve patient (left): magnifying chromoendoscopy showed round regular crypt-opening (CO). Foveola-type microstructure was seen in magnifying NBI. Images from *H. pylori*-associated gastritis patient (middle). Groove-type mucosa was seen in the middle of the endoscopic images. Note that the light blue crest sign, which was a representative endoscopic finding of intestinal metaplasia in magnifying NBI, was seen in the groove-type mucosa. Images from autoimmune gastritis patient (right): foveola-type micromucosal pattern was seen in all endoscopic image fields.

color in the purple corpus mucosa [11]. Kimura analyzed the extent of endoscopic atrophic mucosa and histological atrophic gastritis according to patients' age [18]. He indicated that atrophic gastritis extended upward from the antrum to the cor-pus, along the lesser curvature, and laterally from the lesser curvature to the anterior and posterior wall over time, but not much in the greater curvature [18]. At that time, atrophic gastritis was considered to be part of the normal aging process of
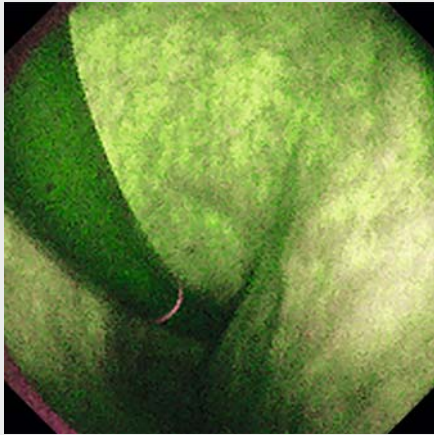
▶ **Video 1** Movies of image-enhanced endoscopic images of corpus mucosa in a Helicobacter pylori (H. pylori)-naïve patient, a patient with H. pylori-associated gastritis, and a patient with autoimmune gastritis.

the gastric mucosa. Later, *H. pylori* was established as a definite pathogen of chronic atrophic gastritis [1]. In comparison to autoimmune gastritis, this lesser curvature predominant endoscopic atrophy was a particular finding in *H. pylori*-associated gastritis. Autoimmune gastritis showed panatrophic change in the corpus mucosa in the present study, which was consistent with a recent, large multicenter observational study [22].

We previously reported that, in *H. pylori*-associated gastritis, groove-type mucosa developed multifocally among foveola-type mucosa in the gastric corpus, and increased in proportion as the area of endoscopic corpus atrophy extended [15]. Likewise, in the present study, patients with *H. pylori*-associated gastritis had varying proportions of groove-type mucosa in the corpus according to size of extent of atrophic mucosa. In contrast, most patients with autoimmune gastritis had only foveola-type micromucosal pattern in the corpus, which was similar to that in patients who were *H. pylori*-naïve, even though there was extensive corpus mucosal atrophy. We explain the difference in micromucosal structure by different histological findings in the gastric mucosa in *H. pylori*-associated and autoimmune gastritis. *H. pylori*-associated gastritis showed diffuse infiltration of mononuclear inflammatory cells in the superficial layer of the lamina propria and neutrophils in the neck of the gastric glands [23, 24] in response to colonization by *H. pylori* on the surface of the foveolar epithelium. Therefore, the surface of the foveolar epithelium may develop regenerative hyperplasia [23]. Moreover, chronic *H. pylori* infection induces genetic alteration in the epithelium, develops intestinal metaplasia [25, 26], and replaces both foveolar and glandular epithelium in the oxyntic mucosa by intestinal-type epithelium [23]. Accordingly, the foveola micromucosal pattern might change to the groove-type pattern in *H. pylori*-associated gastritis. Supporting this speculation, the groove-type mucosa often had a white-bluish fringe of light on the surface of the epithelial

crests (light blue crest) in magnifying NBI images, which are a specific sign of intestinal metaplasia (▶ **Fig. 3**) [12]. In contrast, autoimmune gastritis shows a basal-predominant, chronic inflammatory cell infiltrate in the lamina propria [23, 24], thus the surface of the foveolar epithelium is less involved. Moreover, epithelial metaplasia seen in the early phase of autoimmune gastritis is usually pseudopyloric or pancreatic acinar cell metaplasia of the glandular epithelium, and intestinal metaplasia is not frequently seen until advanced phases of the disease [23, 24]. These histological findings in autoimmune gastritis explain the unchanged foveola micromucosal pattern in magnifying NBI (▶ **Fig. 5**). In support of this hypothesis, the biopsy specimens in the present study showed various grades of intestinal metaplasia that involved the whole mucosal layer in *H. pylori*-associated gastritis. In autoimmune gastritis, glandular atrophy existed but the surface foveolar epithelium looked similar to the normal mucosa and intestinal metaplasia was not seen (▶ **Fig. 4**).
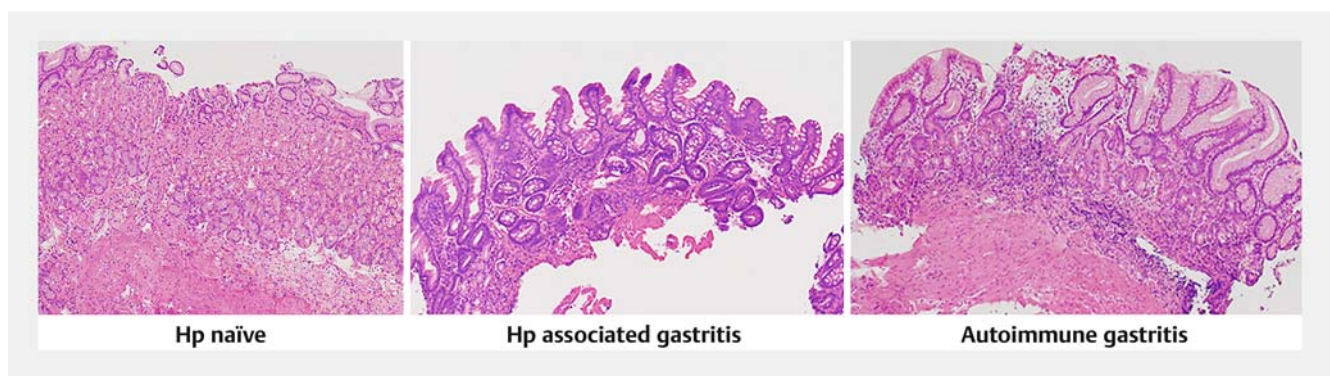
Histological findings of autoimmune gastritis differ according to early, florid and end phases [23, 24]. In our study, the patients with autoimmune gastritis were younger than those with *H. pylori*-associated gastritis. Moreover, in some patients, a small amount of oxyntic gland remained in a biopsy specimen (moderate grade of atrophy). Therefore, we might have evaluated mainly the early to florid phases of mucosal changes in autoimmune gastritis patients. We observed one autoimmune gastritis patient with grove-type micromucosal pattern in the corpus mucosa. In this regard, investigation of autoimmune gastritis in different phases and analysis of IEE findings are needed. Because the prevalence of *H. pylori* infection is declining in Japan and western countries [27, 28], relative prevalence of autoimmune gastritis among patients with chronic atrophic gastritis may increase in the future. Although systematic biopsies are needed for definitive diagnosis of autoimmune gastritis, it is important to suspect the disease during initial endoscopic examination. Our IEE findings show that the foveola-type micromucosal pattern seen in the large atrophic corpus mucosa is useful for early detection of autoimmune gastritis that might be missed by conventional WLI.

Although this was an international study that included Japanese and Swedish patients, all patients with *H. pylori*-associated gastritis were Japanese. Therefore, IEE findings of *H. pylori*-associated gastritis in western patients were not evaluated. *H. pylori*-associated gastritis is usually pangastritis in countries where gastric cancer is highly endemic, but it is confined to the antrum in western countries [23]. So, we assumed that when pangastritis exists in a western patient, autoimmune gastritis is highly suspicious, and confirmation of the >80 % foveola-type micromucosal pattern in the corpus lesser curvature increases level of confidence of the diagnosis. In the present study, we analyzed IEE findings of the corpus mucosa but we consider evaluation of antral gastritis is also useful for differentiation of *H. pylori*-associated and autoimmune gastritis. The corpus mucosa can be involved in both *H. pylori*-associated and autoimmune gastritis, but the antral mucosa is affected only in *H. pylori*-associated gastritis. Previously, we found that *H. pylori*-associated gastritis develops a white villiform micromucosal

▶**Table 3** Histological grade of gastritis in the corpus lesser curvature.

	H. pylori-naïve (n = 7)	*H. pylori*-associated gastritis (n = 21)	Autoimmune gastritis (n = 6)[1]	*P* value
Activity				0.745
▪ Normal	7	20	6	
▪ Mild	0	1	0	
▪ Moderate	0	0	0	
▪ Marked	0	0	0	
Inflammation				< 0.001
▪ Normal	5	0	0	
▪ Mild	2	1	2	
▪ Moderate	0	8	4	
▪ Marked	0	12	0	
Atrophy				< 0.001
▪ Normal	7	1	0	
▪ Mild	0	0	0	
▪ Moderate	0	9	4	
▪ Marked	0	11	2	
Intestinal metaplasia				0.015
▪ Normal	7	6	6	
▪ Mild	0	3	0	
▪ Moderate	0	6	0	
▪ Marked	0	6	0	

[1] A biopsy specimen was not obtained from one autoimmune gastritis patient.

Hp naïve   Hp associated gastritis   Autoimmune gastritis

▶**Fig. 4** Representative histological findings of biopsy specimens taken from the region of interest in a *Helicobacter pylori* (*H. pylori*)-naïve patient (left), *H. pylori*-associated gastritis patient (middle), and autoimmune gastritis patient (right). In *H. pylori*-associated gastritis, foveolar epithelium and fundic glands were replaced by intestinal metaplasia. In autoimmune gastritis, only glandular atrophy but not intestinal metaplasia was seen. The foveolar epithelium became hyperplastic but the structure was similar to that of a *H. pylori*-naïve patient.

pattern in the antrum that has high-grade histological atrophy and intestinal metaplasia [29]. Later, we found that the white color in the villiform micromucosal pattern was caused by presence of LBC and a white opaque substance in magnifying NBI images [30,31]. Analysis of endoscopic findings of the antral

mucosa can further facilitate discrimination of the two types of gastritis.

In this study, we excluded patients in whom *H. pylori* had been eradicated and patients with autoimmune gastritis who had definite (anti-*H. pylori* antibody ≥ 10 U/mL) or possible (anti-*H. pylori* antibody 3–9 U/mL) co-existence of *H. pylori* asso-
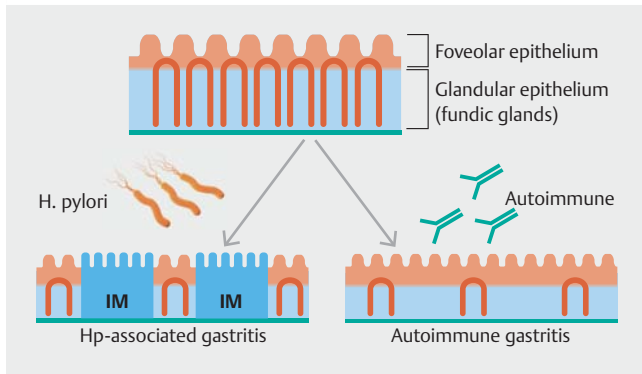
▶ **Fig. 5** Schematic diagram of a possible mechanism for different micromucosal pattern in *Helicobacter pylori* (*H. pylori*)-associated gastritis and autoimmune gastritis. *H. pylori*-associated gastritis develops intestinal metaplasia (IM) and replaces foveolar and glandular epithelium with intestinal-type mucosa. Autoimmune gastritis causes atrophy of glandular epithelia but the structure of foveolar epithelium is minimally altered.

ciated gastritis. A 10-year follow up study demonstrated that *H. pylori* eradication causes slight but gradual improvement of histological atrophy and intestinal metaplasia in the corpus lesser curvature [32], but how the micromucosal pattern in magnifying NBI images alters over the time is unknown. Many studies indicate that substantial numbers of patients with autoimmune gastritis have a current or past *H. pylori* infection [33] and new evidence suggests that some patients with autoimmune gastritis may develop it as a sequelae of chronic *H pylori* infection [34]. However, how both types of chronic gastritis interact is not fully understood [24]. Taking these facts and limited numbers of study subjects into account, we decided to enroll patients with active *H. pylori* infection and patients with sole autoimmune gastritis in this study.

This study had several limitations. First, although it is the largest study to date to systematically investigate IEE findings in f autoimmune gastritis, the number of study subjects was small. Terao et al. reported some characteristic findings of autoimmune gastritis, i.e., remnant oxyntic mucosa, sticky adherent dense mucus and scattered minute whitish protrusions [22], but such findings were not seen in the present study subjects. Accordingly, effect of selection bias was not negligible, and the results should be validated in a large-scale study. Second, we used an AFI system and zoom videoendoscope that are not commonly available in clinical practice. The basis for diagnosis of endoscopic atrophy was established using fiberoptic endoscopy [18]. Therefore, we believe that diagnosis of endoscopic atrophy is practical with high definition WLI videoendoscopy. Although magnifying NBI was used for assessment of micromucosal pattern in our study, two simple classifications, foveola- and groove-types, were assessable with other methods such as near-focus NBI, close observation nonmagnifying NBI, or chromoendoscopy. Third, we did not perform serum anti-parietal cell and anti-intrinsic factor tests in autoimmune gastritis patients. Recently, histological diagnosis of systematic endoscopic biopsy has become more important than serological tests for diagnosis of autoimmune gastritis [24]. We consider that our diagnostic criteria based on clinical manifestations and endoscopic biopsy justify the diagnosis of autoimmune gastritis.

Conclusion

In conclusion, we clarified the different IEE findings between *H. pylori*-associated and autoimmune gastritis, suggesting different pathogenesis of the two diseases. These findings may increase the diagnostic yield of endoscopy for detection of autoimmune gastritis in clinical practice.

Acknowledgements

Competing interests

The authors declare that they have no conflict of interest.

References

[1] Dixon MF, Genta RM, Yardley JH et al. Classification and grading of gastritis. The updated Sydney System. International Workshop on the Histopathology of Gastritis, Houston 1994. Am J Surg Pathol 1996; 20: 1161–1181

[2] Kuipers EJ, Thijs JC, Festen HP. The prevalence of Helicobacter pylori in peptic ulcer disease. Aliment Pharmacol Ther 1995; 9: 59–69

[3] Uemura N, Okamoto S, Yamamoto S et al. Helicobacter pylori infection and the development of gastric carcinoma. N Engl J Med 2001; 345: 784–789

[4] International Agency for Research on Cancer. Schistosomes, liver flukes and Helicobacter pylori. IARC Monographs on the Evaluation of Carcinogenic Risks to Humans. Volume 61. Lyon, France: IARC; 1994: 177–220

[5] Stolte M, Bayerdorffer E, Morgner A et al. Helicobacter pylori and gastric MALT lymphoma. Gut 2002; 50: (Suppl. 03): 19–24. doi:10.1136/gut.50.suppl_3.iii19

[6] Schade SG, Cohen RJ, Conrad ME. Effect of hydrochloric acid on iron absorption. N Engl J Med 1968; 279: 672–674

[7] Irvine WJ, Cullen DR, Mawhinney H. Natural history of autoimmune achlorhydric atrophic gastritis. A 1-15-year follow-up study. Lancet 1974; 2: 482–485

[8] Itsuno M, Watanabe H, Iwafuchi M et al. Multiple carcinoids and endocrine cell micronests in type A gastritis. Their morphology, histogenesis, and natural history. Cancer 1989; 63: 881–890

[9] Kaltenbach T, Sano Y, Friedland S et al. American Gastroenterological Association (AGA) Institute Technology Assessment on Image-Enhanced Endoscopy. Gastroenterology 2008; 134: 327–340

[10] East JE, Vleugels JL, Roelandt P et al. Advanced endoscopic imaging: European Society of Gastrointestinal Endoscopy (ESGE) Technology Review. Endoscopy 2016; 48: 1029–1045

[11] Inoue T, Uedo N, Ishihara R et al. Autofluorescence imaging videoendoscopy in the diagnosis of chronic atrophic fundal gastritis. J Gastroenterol 2010; 45: 45–51

[12] Uedo N, Ishihara R, Iishi H et al. A new method of diagnosing gastric intestinal metaplasia: narrow-band imaging with magnifying endoscopy. Endoscopy 2006; 38: 819–824

[13] Tahara T, Shibata T, Nakamura M et al. Gastric mucosal pattern by using magnifying narrow-band imaging endoscopy clearly distinguishes histological and serological severity of chronic gastritis. Gastrointest Endosc 2009; 70: 246–253

[14] Kawamura M, Abe S, Oikawa K et al. Topographic differences in gastric micromucosal patterns observed by magnifying endoscopy with narrow band imaging. J Gastroenterol Hepatol 2011; 26: 477–483

[15] Kanzaki H, Uedo N, Ishihara R et al. Comprehensive investigation of areae gastricae pattern in gastric corpus using magnifying narrow band imaging endoscopy in patients with chronic atrophic fundic gastritis. Helicobacter 2012; 17: 224–231

[16] Anagnostopoulos GK, Ragunath K, Shonde A et al. Diagnosis of autoimmune gastritis by high resolution magnification endoscopy. World J Gastroenterol 2006; 12: 4586–4587

[17] Yagi K, Nakamura A, Sekine A et al. Features of the atrophic corpus mucosa in three cases of autoimmune gastritis revealed by magnifying endoscopy. Case Rep Med 2012; 2012: 368160

[18] Kimura K. Chronological transition of the fundic-pyloric border determined by stepwise biopsy of the lesser and greater curvatures of the stomach. Gastroenterology 1972; 63: 584–592

[19] Kimura K, Takemoto T. An endoscopic recognition of the atrophic border and its significance in chronic gastritis. Endoscopy 1969; 1: 87–97

[20] Tahara T, Yamazaki J, Tahara S et al. Magnifying narrow-band imaging of gastric mucosal morphology predicts the H. pylori-related epigenetic field defect. Sci Rep 2017; 7: 3090

[21] Nagashima K. A sample size determination tool for the chi-square test for 2 x 2 contingency table. 24.06 2013: Available from (Accessed 2020 Aug 31): https://nshi.jp/contents/js/twofreq/

[22] Terao S, Suzuki S, Yaita H et al. Multicenter study of autoimmune gastritis in Japan: clinical and endoscopic characteristics. Dig Endosc 2020; 32: 364–372

[23] Lauwers GY. Autoimmune gastritis.Greenson JK. Diagnostic Pathology: Gastrointestinal. 2nd ed. Philadelphia, PA: Elsevier; 2016: 136–139

[24] Hall SN, Appelman HD. Autoimmune gastritis. Arch Pathol Lab Med 2019; 143: 1327–1331

[25] Mutoh H, Hakamata Y, Sato K et al. Conversion of gastric mucosa to intestinal metaplasia in Cdx2-expressing transgenic mice. Biochem Biophys Res Commun 2002; 294: 470–479

[26] Rita AB, Alex B. Intestinal metaplasia: a premalignant lesion involved in gastric carcinogenesis. J Gastroenterol Hepatol 2009; 24: 193–201

[27] Shiota S, Murakawi K, Suzuki R et al. Helicobacter pylori infection in Japan. Expert Rev Gastroenterol Hepatol 2013; 7: 35–40

[28] Neumann WL, Coss E, Rugge M et al. Autoimmune atrophic gastritis -pathogenesis, pathology and management. Nat Rev Gastroenterol Hepatol 2013; 10: 529–541

[29] Yamasaki Y, Uedo N, Kanzaki H et al. Investigation of mucosal pattern of gastric antrum using magnifying narrow-band imaging in patients with chronic atrophic fundic gastritis. Ann Gastroenterol 2017; 30: 302–308

[30] Kanemitsu T, Yao K, Nagahama T et al. Extending magnifying NBI diagnosis of intestinal metaplasia in the stomach: the white opaque substance marker. Endoscopy 2017; 49: 529–535

[31] Uedo N, Kanzaki H, Ishinara R. Endoscopic diagnosis of gastric intestinal metaplasia. Gastroenterol Endosc 2014; 56: 1941–1952

[32] Kodama M, Murakami K, Okimoto T et al. Ten-year prospective follow-up of histological changes at five points on the gastric mucosa as recommended by the updated Sydney system after Helicobacter pylori eradication. J Gastroenterol 2012; 47: 394–403

[33] Bergman MP, Faller G, D'Elios MM et al. Gastric autoimmunity.Mobley HLT, Mendz GL, Hazell SL. Helicobacter pylori: Physiology and Genetics. Washington, DC: ASM Press; 2001: 429–440

[34] Minalyan A, Benahmmou J, Artashesyan A et al. Autoimmune atrophic gastritis: current perspectives. Clin Exp Gastroenterol 2017; 10: 19–27